

Selective pharmacophore design for α_1 -adrenoceptor subtypes

Iain J.A. MacDougall, Renate Griffith *

School of Environmental and Life Sciences, The University of Newcastle, Australia

Received 15 September 2005; received in revised form 1 December 2005; accepted 1 December 2005

Available online 6 January 2006

Abstract

α_1 -Adrenoceptors are G-protein coupled receptors found in a variety of vascular tissues and responsible for vasoconstriction. Selectivity for each of the three subtypes is an important consideration in drug design in order to minimise the possibility of side effects. Using Catalyst[®] we developed ligand-based pharmacophores from $\alpha_{1a,b,d}$ -selective antagonists available in the literature using three separate training sets. Four-feature pharmacophores were developed for the α_{1a} and α_{1b} subtype-selective antagonists and a five-feature pharmacophore was developed for the α_{1d} subtype-selective antagonists. The α_{1a} pharmacophore represents both class I and II compounds with good predictivity for other compounds outside the training set as well. The α_{1b} pharmacophore best predicts the activity of prazosin analogues as these make up the majority of α_{1b} -selective antagonists. Unexpectedly, no positive ionisable feature was incorporated in the α_{1b} pharmacophore. The α_{1d} pharmacophore was based primarily on one structural class of compounds, but has good predictivity for a heterogeneous test set. Preliminary docking studies using AutoDock and optimised α_1 -adrenoceptor homology models, conducted with the antagonists prazosin (**32**) and **66**, showed good agreement with the findings from the pharmacophores.

© 2005 Elsevier Inc. All rights reserved.

Keywords: α_1 -Adrenoceptor subtypes; Selectivity; Pharmacophore; Antagonist; Docking

1. Introduction

The human adrenergic receptors (ARs) are members of the superfamily of G-protein coupled receptors (GPCRs), all of which have seven antiparallel transmembrane helices. The nine known ARs fall into three classes: α_1 ; α_2 ; and β , each consisting of three subtypes. α_1 -ARs are widely distributed throughout the body and mediate a number of physiological responses of the sympathetic nervous system. Binding of the endogenous ligands adrenaline or noradrenaline to the membrane-bound receptor from the extracellular side initiates an intracellular signalling cascade. α_{1a} -AR occurs in heart and vascular tissue where it regulates arterial blood pressure in prostate and urinary tissues, mediating contraction of the tissues, and is a target for treatment of benign prostatic hyperplasia (reviewed in [1]). α_{1b} -AR enables contraction of heart, vascular, prostate and spleen tissues, while α_{1d} -AR is found in various vascular tissues including the renal artery (reviewed in [1]).

ARs have been implicated in a number of diseases and as such are valuable targets for drug discovery. Of all drugs currently used clinically, approximately 50% are targeted towards GPCRs [2]. ARs are also often responsible for side effects of drugs targeting other GPCRs such as dopamine and serotonin receptors. Due to the similarity in structure within the adrenoceptor family, specificity of antagonists towards their intended target is a crucial issue. Antagonists with $>100\times$ selectivity for α_{1a} over both α_{1b} and α_{1d} have been known since the mid-1990s and recently a number of highly selective α_{1d} antagonists have been published. For α_{1b} the most selective compound is (+)-cyclazosin with 25-fold selectivity over α_{1d} and approximately 100-fold selectivity over α_{1a} [3].

We have previously investigated AR subtype specificity using ligand-based computational methods [4,5] and other groups have also developed pharmacophores for α_1 -AR subtypes. General α_1 pharmacophores have been developed previously [6,7], but few address the subtype-selectivity issue. The general α_1 -AR pharmacophore developed by Barbaro et al. [6] was based on a single family of pyridazinone derivatives as well as arylpiperazine-containing compounds and was subsequently elaborated on to create an α_{1d} subtype-specific pharmacophore [8]. Li et al. [9] developed an α_{1a} pharmacophore based on a diverse training set and with good results, but

* Corresponding author at: Biological Sciences Building, Callaghan, NSW 2308, Australia. Tel.: +61 2 49216990; fax: +61 2 49216923.

E-mail address: Renate.Griffith@newcastle.edu.au (R. Griffith).

did not account for selectivity over the other subtypes. Others have further attempted to elucidate the mechanisms of subtype selectivity by dividing α_{1a} antagonists into subclasses and developing pharmacophores for each class [10].

The pharmacophores published here incorporate a wide variety of antagonists for each of the three α_1 -AR subtypes and include the most recently published ligands. Previously published pharmacophores, including ours, have been developed without taking into account the selectivities of the antagonists. By limiting the training sets to include only those antagonists with a high degree of selectivity over the other subtypes, we have been able to weight the pharmacophores so that they represent high selectivity and high affinity, rather than solely high affinity.

2. Methods

2.1. General methodology

All pharmacophores were produced using the Catalyst[®] program, version 4.9 (Accelrys Inc., San Diego, CA, USA). Docking of antagonists into minimised homology models of receptors was performed using the program AutoDock, version 3.05 [11–13].

2.2. Training set selection

Training sets for each subtype were compiled from published data pertaining to antagonists of α_1 -ARs [8,14–32]. K_i values were taken for those compounds, which had been subjected to competition assays using recombinant receptors expressed in cell lines, rather than from tissue extracts. K_i was used as Catalyst defines the compound with the lowest value of the training set as the most active. For α_{1a} and α_{1d} pharmacophores only those compounds that exhibited >100-fold selectivity over α_{1b} and >40-fold selectivity over α_{1a}/α_{1d} (as calculated by the ratio of K_i values) were included in the training set. The ranges of K_i values for α_{1a} and α_{1d} training sets did not exceed the recommended 3.5 orders of magnitude [33], however there were at least three compounds within each order of magnitude. To avoid redundancy of information, training sets were refined by removing similar compounds with similar affinities. Compounds where reduction in affinity was suspected to have resulted from an increase in steric bulk were also removed, because in its default mode, Catalyst does not consider features, which contribute in a negative way towards activity, such as steric clashes between a ligand and a binding site. Training sets are summarised in Table 1.

Table 1
Summary of training set composition for α_{1a} , α_{1b} and α_{1d} selective antagonists

Pharmacophore	Number of compounds included	Number of actives	Range of activity, K_i (nM)	Order of magnitude
α_{1a}	27	5	0.16–98	2.79
α_{1b}	21	6	0.3–794	3.32
α_{1d}	20	5	0.11–35.5	2.51

Conformers of each compound were generated in Catalyst using a 20 kcal/mol range limit, as recommended for pharmacophore generation [33], and the best search option. For compounds where the stereochemistry was not known, all possible conformers were generated. This was not necessary for any compounds in the α_{1d} training set, and in the α_{1b} training set only one compound with low affinity had undefined stereochemistry. Six compounds were affected in the α_{1a} training set, none of them with high affinity. The mapping of the two enantiomers to the final pharmacophore was checked for one compound and it was found that both enantiomers exhibited equally good fits. Catalyst uses the poling algorithm in order to ensure the conformational space is effectively sampled [34–36]. For each compound the number of conformers generated was less than the maximum of 255 that can be processed during pharmacophore generation [33].

2.3. Hypothesis generation

Hypotheses were generated using the HypoGen algorithm in Catalyst with the feature options of H-bond acceptor (HBA), H-bond donor (HBD), hydrophobic (aromatic)(Har), hydrophobic (aliphatic)(Hal) and positive ionisable (PI). The PI feature represents atoms, which have the ability to be protonated and thus become positively charged, e.g. an sp^3 hybridised nitrogen. In the cases of α_{1a} and α_{1d} , where the PI feature was quite often apparent in resultant hypotheses, the presence of exactly one PI feature per hypothesis was required to reduce the complexity of the problem, ensuring the entire hypothetical space was sampled. The rationale for this is based on the interaction between a positive region of the ligand with the acid group of a conserved aspartate residue in the binding pockets of α_1 -ARs being thought to be crucial in binding of small molecules [37–39]. Har and Hal features were chosen to allow differentiation between aromatic (π – π) interactions and more generic hydrophobic interactions. Uncertainty values were calculated for each compound as the ratio between the maximum and minimum affinity values, as specified by the reported experimental error, where experimental errors were unavailable the default uncertainty value of 3 was used.

2.4. Generation of homology models

Homology models of α_1 -ARs were based on a crystal structure of bovine rhodopsin (1GZM) obtained from the Protein DataBank (<http://www.rcsb.org/pdb>). This template was chosen as it gave the best resultant homology models in terms of secondary and tertiary structure validation. Sequence alignments were created with ClustalW version 1.74 (<http://www.bork.embl-heidelberg.de:8080/Alignment/alignment.html>) and further refined in Swiss-PDBViewer [40–42] with close reference to highly conserved residues within transmembrane helices and loops (Fig. 1; reviewed in [43]). Within the transmembrane helices, where the binding pocket lies, the three α_1 -AR subtypes have approximately 25% identity and 55% similarity with the template sequence. Homology models were created using the optimise mode of SwissModel

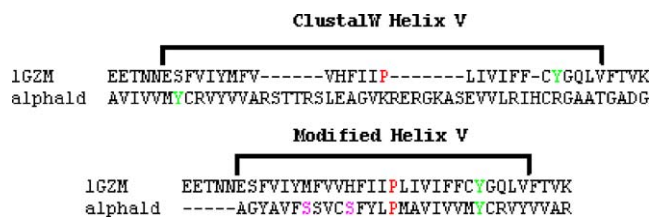


Fig. 1. ClustalW and modified alignments of α_{1d} helix V. The black bar represents the rhodopsin helix V and what would be the resultant α_{1d} helix V in the homology model. In the modified alignment the conserved proline and tyrosine residues are aligned and the binding site serine residues are within the helix.

[40–42]. In this program the loops are modelled in an automated fashion with no user input. For the α_{1a} and α_{1b} models the disulphide bridge between helix III and extracellular loop II was not built by SwissModel and had to be added. Homology models were imported into DSModeling1.1 (Accelrys, San Diego, CA, USA) for refinement. Atom types were checked, hydrogens and partial charges were added from a library. Structures were minimised using the Steepest Descent and Powell algorithms as implemented in the CHARMM forcefield. Disulphide bridges were constructed where necessary, and the loop region minimised with the rest of the protein constrained. For further refinement, the backbone was initially constrained during minimisation until the maximum derivative was less than 0.01 kJ/mol Å, then all atoms were minimised without constraints until the maximum derivative was less than 0.01 kJ/mol Å. Structures were then solvated with explicit TIP3 water molecules in the internal region of the 7TM helical bundle. The structures were further minimised in the presence of explicit waters until the maximum derivative was less than 0.01 kJ/mol Å using a similar protocol as above.

2.5. AutoDock

All AutoDock runs were conducted using AutoDock version 3.05 [11–13] on a Silicon Graphics Fuel workstation using an IRIX64 Release 6.5 operating system. Water molecules were removed prior to docking procedures. Grids were constructed with 80 x , y and z grid points with 0.375 Å grid point spacing, centred on a carbonyl oxygen of the conserved Asp residue in the ligand binding site (α_{1a} -Asp106, α_{1b} -Asp125, α_{1d} -Asp176). The grid encompassed the entire ligand binding site and part of the extracellular region. Grid maps were calculated with atom types C, A, N, O, H (where A represents aromatic carbons) and electrostatic energies. Ligands were docked using the Lamarckian genetic algorithm with local search (GA-LS), with the initial position of the ligand at the centre of the grid. For each of the 250 runs with a maximum number of energy evaluations set at 2,500,000, step sizes of 2 Å for translation and 50° for rotation were chosen. The maximum number of 27,000 generations was generated on a population of 50 individuals. Operator weights for rate of gene mutation, rate of crossover and elitism were set to 0.02, 0.8 and 1, respectively. The 250 poses reported at the end of each docking experiment were clustered by RMSD (2 Å). All large clusters with low

docking energies were inspected visually. All poses docked outside the helix bundle were discarded.

3. Results and discussion

Catalyst produces hypotheses by assigning and arranging chemical features such as H-bond acceptor, hydrophobic and positive ionisable to a training set of molecules according to the relationship between their structures and their affinity values. During the constructive phase of hypothesis generation, all possible patterns of features that can be found in the two most active compounds are enumerated [44]. A maximum of six other compounds within the highest affinity tier are checked for their fit to the hypotheses and only those hypotheses which fit these compounds are kept. The highest affinity tier is calculated using the uncertainty value, which is based on the error of the experimentally-derived K_i value [44]. Table 1 indicates the number of compounds seen as active by Catalyst in each training set. If the affinities of the training set span more than 3.5 orders of magnitude, then those compounds in the lowest tier of affinity are used in the subtractive phase to discard hypotheses, which are found in inactive, as well as active, compounds. During the optimisation phase the hypotheses are refined by randomly translating, rotating and adding/discarding features, by default the 10 statistically best hypotheses are kept [44].

The statistical validity and rank of hypotheses generated by Catalyst is measured by the following parameters: (1) correlation (R^2) between real and estimated affinity values, which lies between 0.0 and 1.0 where 1.0 is perfect correlation; (2) configuration cost, which describes the total hypothetical space and should be less than 17 to ensure all possibilities have been considered; (3) the difference in total costs between generated hypotheses and the null hypothesis, which should be >60 bits for a >90% statistical probability that a hypothesis represents a real correlation with biological activity. The total cost represents the combined error of estimation as calculated by the ratios between experimental and estimated activities, the deviation of the feature weights from the ideal weight (2.0), and the complexity of the hypothetical space; the null cost pertains to a hypothesis with no features which assumes there is no relationship between structure and activity for the entire training set [45].

Catalyst also allows the generation of negative control hypotheses whereby it randomly reassigns the affinity values within a training set using Fischer randomization and generates new spreadsheets. It then calculates the statistical significance of the actual hypotheses generated by comparing the total costs of the actual hypothesis and the randomized spreadsheets. A confidence level of 95%, 98% or 99% can be attained depending on whether 19, 49 or 99 random spreadsheets are generated. In our case 19 random spreadsheets were generated for each training set, giving a confidence level of 95% for the results. The α_{1a} pharmacophore had a statistical significance of 90%, α_{1b} had a significance of 65%, while α_{1d} had a significance of 95%. The lower significance of the α_{1b} model may be due to the amount of variety among compounds in the

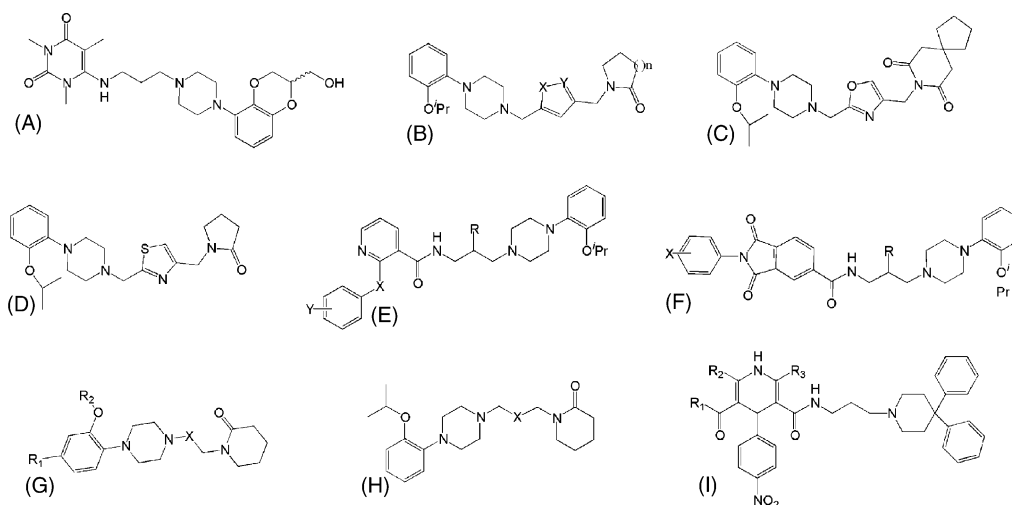
top tier of activity. The α_{1a} and α_{1d} training sets have more similarity among the compounds seen as actives by Catalyst than the α_{1b} training set.

4. Hypothesis analysis

4.1. α_{1a} Pharmacophore model

Fig. 2 (part I) shows the compounds in the training set for the α_{1a} hypothesis generation. Hypotheses were initially generated with H-bond acceptor (HBA), H-bond donor (HBD), hydro-

phobic (aliphatic)(Hal), hydrophobic (aromatic)(Har) and positive ionisable (PI) as possible features. The configuration value was found to be greater than 18, meaning that less than half of the whole hypothetical space had been sampled. As none of the 10 hypotheses generated contained HBD and the PI feature was known to be essential, the generation was repeated without HBD as a possible feature and with there having to be at least one PI feature. These measures were found to reduce the configuration value to less than 17, meaning the entire hypothetical space had been sampled. However, it was found that combinations other than HBA, Hal, Har and PI or HBA,



Compound	K _i (nM)	Structure	Selectivity / α_{1b}	Selectivity / α_{1d}
B8805-033(1)[13]	19.5	A	354	166
2[20]**	1.1	B X=O Y=N n=1	2720	60
3[20]**	8.4	B X=O Y=N n=2	>595	174
4[20]**	82	C	>61	50
5[21]**	0.5	B X=S Y=C n=2	768	184
6[20]**	0.9	D	4522	112
7[25]*	1.54	E R=OH X=O Y=H	579	137
8[25]*	1.0	E R=OH X=O Y=4-Cl	834	73
9[25]*	0.52	E R=OH X=O Y=4-CH ₃	1797	40
10[25]*	2.38	E R=OH X=O Y=4-OCH ₃	804	55
11[25]*	2.6	E R=OH X=S Y=4-Cl	310	116
12[25]*	0.79	E R=S-OH X=O Y=H	800	104
13[25]*	0.48	E R=S-OH X=O Y=4-CH ₃	593	102
14[24]*	1.02	F R=S-OH X=3-F	>1960	186
15[24]*	0.23	F R=S-OH X=4-OCH ₃	>7610	539
16[24]*	0.29	F R=S-OH X=4-CH ₃	>5690	186
17[24]*	0.46	F R=S-OH X=4-OH	>4350	298
18[24]*	0.16	F R=H X=4-CH ₃	>12500	231
19[27]	98	G R ₁ =H R ₂ =CH ₃	102	102
20[27]	8.7	G R ₁ =H R ₂ = <i>i</i> -Pr	5301	40
21[27]	83	G R ₁ =F R ₂ = <i>i</i> -Pr	120	54
22[27]	0.66	G R ₁ =H R ₂ = <i>i</i> -Pr	15152	121
23[28]**	2.1	H X=	1864	84
24[28]**	79	H X=	>127	>127
25[28]**	3.8	H X=	1172	72
SNAP-5150(26)[19]*	1.9	I R ₁ =NH ₂ R ₂ =CH ₃ R ₃ =CH ₃	174	211
SNAP-5399(27)[19]*	0.65	I R ₁ =OCH ₃ R ₂ =CH ₂ CH ₃	498	971

Fig. 2. (part I) Structures of α_{1a} -AR training set antagonists. (part II) Structures of α_{1b} -AR training set antagonists. Note: Prazosin is not part of the α_{1b} -AR training set. (part III) Structures of α_{1d} -AR training set antagonists. * class I antagonists, ** class II antagonists.

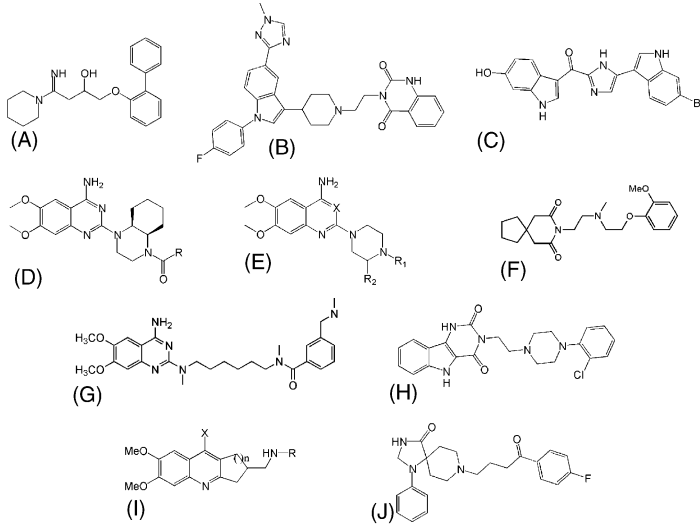
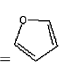
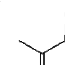
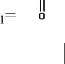
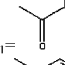
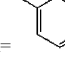
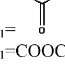
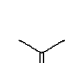
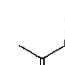
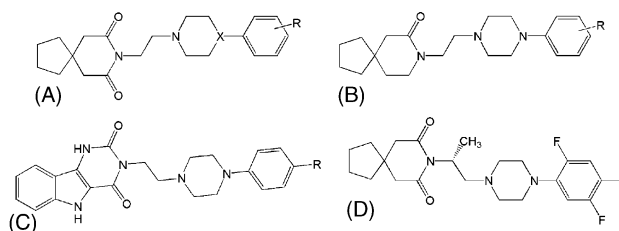
				
Compound	K_i (nM)	Structure	Selectivity $/\alpha_{1a}$	Selectivity $/\alpha_{1d}$
AH11110A(28)[22]	76	A	33	36
29 [14]**	0.39	B	3	8
bromotopsentin(30)[30]	794	C	16	unknown
cyclazosin(31)[17]	0.13	D 	92	25
prazosin(32)	N/A	D 	N/A	N/A
doxazosin(33)[19]	1	E $R_1 =$  $R_2 = H$ $X = N$	3	4
34 [18]	0.38	E $R_1 =$  $R_2 = H$ $X = N$	4	2
35 [26]	8.21	D $R =$ 	>122	2
36 [49]	0.16	F	2	2
37 [29]	25	G	33	10
38 [29]	3.5	E $R_1 = H$ $R_2 = CONHC(CH_3)_3$ $X = N$	486	21
39 [29]	2	E $R_1 =$  $R_2 = CONHC(CH_3)_3$ $X = N$	210	17
40 [32]	0.3	E $R_1 = COOCH_2Ph$ $R_2 = CONHC(CH_3)_3$ $X = N$	6	9
41 [8]**	2.57	E $R_1 =$  $R_2 = H$ $X = C$	2	2
42 [31]	79.4	H	2	3
43 [31]	7.41	I $X = NH_2$ $n = 1$	39	3
44 [31]	12.59	I $R = CPh_2-CH_3$ $X = NH_2$ $n = 2$	3	2
45 [31]	8.91	I $R = CPh_3-CH_3$ $X = NH_2$ $n = 2$	10	2
46 [31]**	39.81	I $R = CH_2CH_2OPh$ $2,6-OMe$ $n = 2$	25	5
47 [31]	295.1	I $X = OH$ $n = 2$	9	4
sipiperone(48)[16]	0.5	J	16	26
terazosin(49)[19]	2	E $R_1 =$  $R_2 = H$ $X = N$	3	1.25

Fig. 2. (Continued).

Hal and PI gave either large errors for the highest activity compounds or pseudo-features. A pseudo-feature is a feature of a hypothesis that maps only to the highest affinity compound and to no other compound in the training set. This meant that of the 10 resultant hypotheses, very few were statistically valid and therefore could not be considered for analysis. To avoid the problem of having too few results for consideration, hypotheses

were generated with the restrictions HBA = 1, Hal = 1, Har = 0/1 and PI = 1, resulting in statistically valid hypotheses. The most statistically favourable pharmacophore consisted of an HBA and Har feature in close proximity, along with PI and Hal features. This hypothesis had a correlation of >0.95 between the estimated values for the compounds in the training set and their experimentally described affinities, as well as >60 bits



Compound	K_i (nM)	Structure	Selectivity α_{1a}	Selectivity α_{1b}
50[26]	4.32	A R=H X=N	777	61
51[26]	0.83	A R=4-Cl X=N	665	105
52[26]	2.02	A R=3-Cl X=N	>495	109
53[26]	0.91	A R=2-F X=N	>1099	69
54[26]	0.93	A R=2-CN X=N	230	50
55[26]	1.6	A R=2-Br X=N	235	76
56[26]	0.13	A R=2,5-Cl ₂ X=N	985	76
57[26]	0.14	A R=2,5-F ₂ X=N	965	42
58[26]	2.38	A R=2-F, 5-CH ₃ X=N	>420	50
59[26]	7.56	A R=2-F, 5-CF ₃ X=N	>132	>132
60[26]	0.37	A R=2-CH ₃ , 5-Cl X=N	514	72
61[26]	0.2	A R=2-CN, 5-Cl X=N	2516	85
62[26]	0.18	A R=2-Cl, 5-F X=N	598	56
63[26]	3.66	A R=H X=C	>273	68
64[26]	0.54	B R=2-Cl	162	67
65[26]	0.37	B R=2-OMe	147	149
66[26]	0.11	B R=2,5-Cl ₂	386	72
67[8]**	35.5	C R= <i>i</i> -Pr	363	280
68[8]**	20	C R=C(CH ₃) ₃	unknown	unknown
SNAP-8719(69)[23]	1.6	D	184	119

Fig. 2. (Continued).

difference between total cost and the null hypothesis cost. The pharmacophore is summarised in Table 2. Of the 10 highest affinity compounds only compounds 8 and 9 had predicted affinities with errors of >3. The remaining nine hypotheses were not considered due to either large errors for the top compound or similarity with the first hypothesis. Fig. 3A and B show the highest affinity compound (18) mapped onto the α_{1a} pharmacophore. The PI feature (red) maps consistently to N1 of the piperazine ring of structures in the training set.

Klabunde and Evers produced pharmacophores for α_{1a} by dividing high-affinity antagonists into two classes based on the spacing of aromatic features with regard to the PI nitrogen. Class I antagonists are classified by a PI nitrogen positioned 2–3 bond lengths from an aromatic ring and 6–7 bond lengths from a second aromatic ring. Class II antagonists exhibit two aromatic rings, both positioned 2–4 bond lengths from a PI nitrogen. Our training set of α_{1a} selective antagonists contains both classes of compounds, together with compounds, which do not fit in either class (see Fig. 2, part I). Of the compounds in this training set with a K_i of less than 1 nM, eight are class I, two are class II and one could not be classified, but is similar to

class I. Our α_{1a} pharmacophore appears to favour class I compounds in terms of mapping the PI feature, which is not unexpected as the two highest affinity compounds are class I. Of the 10 highest affinity compounds in the training set, all class I antagonists map to the PI, whereas the remaining compounds do not. However, only the three highest affinity compounds map all four features with the HBA feature being missed by five of the class I compounds.

4.2. α_{1b} Pharmacophore model

The training set for the α_{1b} subtype consisted of compounds that exhibited any selectivity over both α_{1a} and α_{1d} subtypes in competition assays (Fig. 2, part II). These compounds consist primarily of prazosin analogues, which cannot be classified into class I or II as the α_{1a} antagonists have been. Hypotheses were generated with HBA, HBD, Hal, Har and PI as possible features. It has previously been noted that Catalyst does not recognise a PI feature in prazosin analogues by default [10]. To counteract this problem, the N1 nitrogen of the quinazoline ring was manually protonated, in accordance with the findings of De Benedetti et al. [46]. Despite this measure, the PI feature was not part of any hypothesis developed for the α_{1b} subtype. As the configuration value was less than 17, meaning that the entire hypothetical space had been sampled, no restrictions were placed on features. Of the hypotheses generated with prediction errors of <5 for the two most active compounds, the first consisted of 2× HBA, Hal and Har, while the next three consisted of HBA, Hal and Har features. The four-feature hypothesis exhibited a correlation of 0.95 with the training set

Table 2
Summary of pharmacophore statistics and composition

Pharmacophore	RMS	R^2	Feature composition	Statistical significance
α_{1a}	3.37	0.96	HBA, Hal, Har and PI	90%
α_{1b}	2.08	0.95	2× HBA, Hal and Har	65%
α_{1d}	1.57	0.91	HBA, 2× Hal, Har and PI	95%

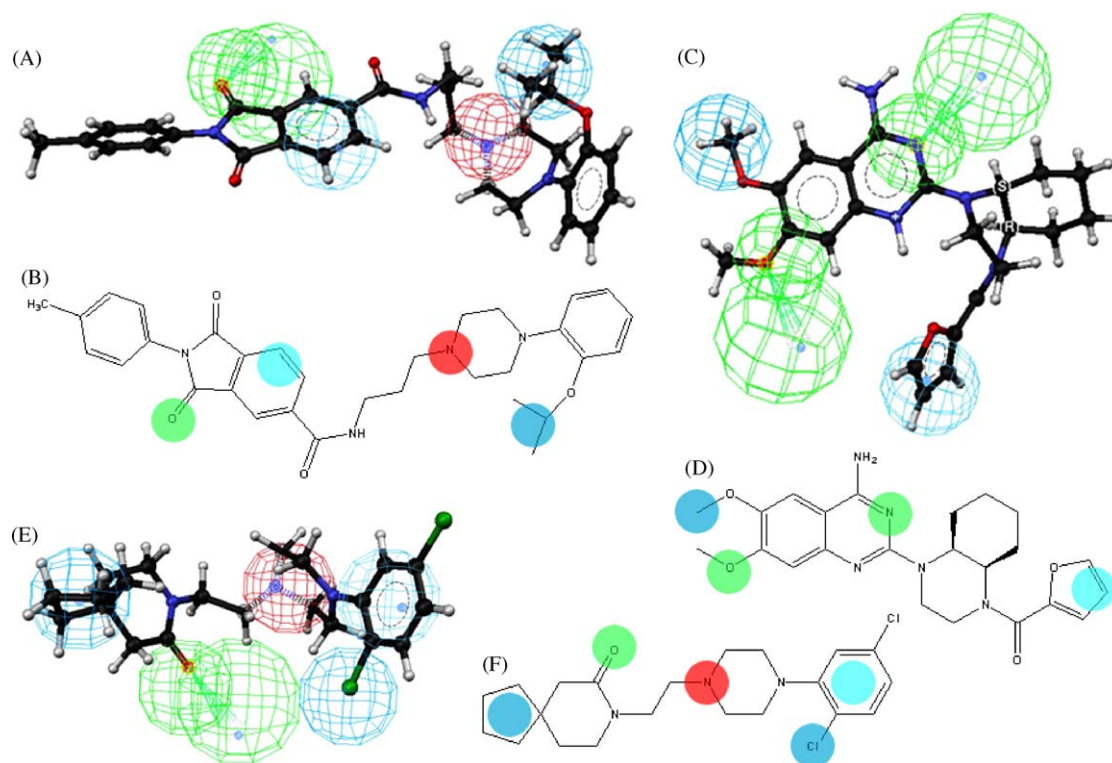


Fig. 3. Pharmacophore mappings of the highest affinity compound for each training set. Mesh spheres represent the three-dimensional location constraints for each feature, HBA features have two spheres to represent directionality of the feature. The coloured spheres correspond to the pharmacophoric features in both three-dimensional and two-dimensional representations with the following colours: green, HBA; light blue, Har; dark blue, Hal; red, PI. (A) and (B) 3D and 2D representations of the α_{1a} pharmacophore mapped onto **18**. (C) and (D) 3D and 2D representations of the α_{1b} pharmacophore mapped onto **31**. (E) and (F) 3D and 2D representations of the α_{1d} pharmacophore mapped onto **66**.

and was chosen as the most likely hypothesis to represent specificity over the other two subtypes. The total cost of this hypothesis was >60 bits different to the null hypothesis cost. Fig. 3C and D show the most active compound, cyclazosin (**31**), mapped onto the α_{1b} pharmacophore. Both HBA and the Hal features map to the planar general piperaziny-6,7-dimethoxyquinazoline structure of the prazosin analogues. The Har feature maps to an aromatic ring present in the top six prazosin analogues as well as in spiperone.

4.3. α_{1d} Pharmacophore model

A training set was developed for the α_{1d} subtype consisting of compounds exhibiting >100-fold selectivity over α_{1a} and >40-fold selectivity over α_{1b} (Fig. 2, part III). Two compounds in this training set can be classified as class II antagonists. As all others contain only one aromatic ring, they cannot be classified according to the Klabunde and Evers classification. Hypotheses were generated with HBA, HBD, Hal, Har and PI as possible features, with one PI feature required in the hypothesis to reduce the configuration value below 17. Of the 10 hypotheses generated, nine contained HBA, 2 \times Hal, Har, PI; and one was missing the second Hal feature. The top ranking hypothesis exhibited a correlation value of 0.91 and >60 bits difference between total cost and the null hypothesis cost and this was chosen as the α_{1d} pharmacophore. As all but two compounds in this training set, both with lower affinity, were structurally

related to BMY-7378, we believe this to be the reason for the ability of Catalyst to directly generate a five-feature hypothesis. In our previously published α_{1d} pharmacophore [5], BMY-7378 was excluded from the training set on the basis of its similarity to SNAP-8719, however it seems that this structural family provides good selectivity over both other subtypes. Of the top nine compounds, all of which are within this structural family, seven map to all five features. Compound **57** misses the PI feature in the best fit but can be fitted to the PI feature with little penalty to the estimated affinity value: 0.69 \rightarrow 1.5. Compound **64** misses the HBA feature but can be fitted to all five features with an increase of estimated affinity value from 0.67 to 2.5. Fig. 3E and F show the highest affinity compound (**66**) mapped onto the α_{1b} pharmacophore. When compared with our previous pharmacophore, the new pharmacophore has two additional hydrophobic features, one adjacent to the aromatic ring, the other mapping to the five membered spiro ring.

4.4. Comparison and validation of pharmacophores

Each pharmacophore was regressed against the training sets for the other two subtypes within Catalyst. Table 3 shows the correlation values for each regression. This table shows that while each pharmacophore showed a high correlation to its own dataset, there was little correlation between the pharmacophores and datasets for other subtypes. To ensure that the low correlation was because of structural differences to do with

Table 3
Cross-validation of pharmacophores against all training sets

Pharmacophore	Training set		
	α_{1a}	α_{1b}	α_{1d}
α_{1a}	0.95	0.58	0.78
α_{1b}	No correlation	0.95	No correlation
α_{1d}	No correlation	No correlation	0.91

Each pharmacophore was regressed against the training sets for the other two subtypes.

subtype selectivity, rather than simply poor correlation to any dataset of compounds not in the training set, each pharmacophore was regressed against test sets for each subtype. Where possible, test sets included a variety of structural families with compounds of different activity and selectivity.

Table 4 shows the predictive power of the α_{1a} pharmacophore for α_{1a} selective antagonists and the α_{1d} pharmacophore for α_{1d} selective antagonists. As all available α_{1b} selective antagonists were included in the training set, no test set could be prepared. The α_{1a} test set consisted of 15 antagonists from various structural families and with varying degrees of affinity and selectivity [15,19,25,47–52]. It appears from the test set that our pharmacophore is best able to predict the affinities of α_{1a} antagonists that fall into either class I or II. Our pharmacophore is least able to predict those antagonists which cannot be classified either because they do not have two aromatic rings, or because the number of bond lengths between aromatic rings and the positively ionisable nitrogen falls outside the parameters for classification. The median error of prediction for the entire training set is 9.77, while for class I and II antagonists only, the median error is 6.74. The α_{1d} test set

consisted of 15 antagonists from various structural families [8,19,26,53–55]. The median error value of 5.25 indicates that this pharmacophore is adept at predicting the experimentally-derived affinity values for a variety of α_{1d} antagonists, despite the low level of variety within the α_{1d} training set. This is a surprisingly good result and indicates that our α_{1d} pharmacophore is quite accurate for predicting affinity towards the α_{1d} -AR, which could be useful for database searching in future.

Inspection of the datasets indicates that one reason for subtype selectivity is the size of the antagonist. The average molecular weights of the training sets are as follows: α_{1a} , 485; α_{1b} , 443; α_{1d} , 400. From this it can be proposed that α_{1a} has the largest binding pocket of the three subtypes and α_{1d} has the smallest. This type of steric selectivity may explain why it is relatively easy to obtain selectivity for α_{1a} or α_{1d} while difficult for α_{1b} . It is also significant that compounds showing α_{1b} selectivity are almost exclusively prazosin analogues. The inability of Catalyst to identify a positively ionisable nitrogen in the quinazoline ring has been previously discussed [4]. In our case, despite the presence of a protonated nitrogen at the N1 position of the quinazoline ring, which is mapped as a PI feature, PI features were never observed in hypotheses generated.

The α_{1a} and α_{1d} pharmacophores fit antagonists, which are in fairly extended conformations, but with a kink in the region of the N1 nitrogen of the piperazine ring. A difference between them is that the α_{1a} antagonists tend to extend beyond the pharmacophoric features, whereas the features of the α_{1d} pharmacophore fit to the extremities of the compounds. In comparison, the α_{1b} pharmacophore requires the prazosin analogues to be of a more folded conformation. Fig. 3C and D show that while the Har feature corresponds to a region of the

Table 4
Summary of the predictive power of α_{1a} and α_{1d} pharmacophores for test sets of selective antagonists. The error is calculated as the ratio between experimentally-derived affinities and affinities predicted by Catalyst

α_{1a}				α_{1d}			
Compound	Measured	Estimate	Error	Compound	Measured	Estimate	Error
70 [19] ^a	0.15	1.1	7.33	85 [26]	16.38	0.71	23.1
71 [49] ^b	0.603	0.7	1.16	86 [19]	6.3	1.2	5.25
72 [50] ^b	0.27	1.3	4.81	87 [55]	25	11	2.27
73 [27] ^a	129	3	43	88 [8]	0.63	28	44.44
74 [48]	5.01	110	21.96	89 [8]	125.9	22	5.72
75 [19] ^b	0.4	4.6	11.5	90 [54]	5.2	25	4.81
76 [47] ^b	0.41	2.3	5.61	91 [54]	63	0.57	110.5
77 [16] ^b	0.2	1.2	6	92 [49]	16.22	36	2.22
78 [15] ^a	4.37	110	25.17	93 [49]	199.53	27	7.39
79 [51] ^b	1.13	0.8	6.15	94 [53]	0.31	3.2	10.32
80 [15]	208.9	1.3	160.7	95 [8]	6.92	8.2	1.18
81 [25] ^a	62.7	0.51	122.9	96 [26]	0.67	1.3	1.94
82 [52] ^b	0.09	0.88	9.77	97 [54]	0.8	1.4	1.75
83 [52] ^b	0.51	0.84	1.65	98 [26]	2.9	4.4	1.52
84 [19]	4	110	27.5	99 [53]	0.25	7	28
Median			9.77	Median			5.25
Median (I,II)			6.74				

References are in parentheses. Affinities are given as K_i values in nM.

^a Class I antagonists.

^b Class II antagonists.

2D structure that is distal to the other features, in the 3D pharmacophore the Har feature lies quite close to the other features.

5. Homology modelling and docking results

5.1. Homology model construction

The homology between the α_1 subtype sequences and bovine rhodopsin sequence ranges between 19–23% and 40–45% for similarity. The transmembrane helices alone exhibit 23–26% identity and 51–55% similarity. α_{1a} has the highest level of identity and similarity with bovine rhodopsin, possibly due to the fact that α_{1a} has the smallest intracellular loop III of the three subtypes. Sequence alignments were created using ClustalW version 1.74 and further manipulated to take into account residues conserved among GPCRs. Fig. 1 illustrates the importance of manually adjusting the alignment to take into account these residues. Using the ClustalW alignment would have resulted in loops in helix V and an inappropriate positioning of two serine residues important in ligand binding. By adjusting the alignment, conserved proline and tyrosine residues are aligned and the serine residues are now positioned facing into the binding pocket where they can interact with ligands.

Model quality was assessed using validation tools implemented by the PROCHECK program [56]. Ramachandran plot

analysis indicated that 91–95% of all backbone dihedral angles for optimised models of the three subtypes lay in the allowed regions, compared with 98% for optimised rhodopsin structure. Considering the transmembrane helices only, 94–96% of backbone dihedral angles lay in the allowed regions for the optimised models, compared with 98% for optimised rhodopsin. In all three models the universally conserved aspartate residue and two conserved serine residues implicated in ligand interaction were positioned facing the binding pocket such that interactions with ligands could occur. A saltbridge between helices III and VI involving the E/DRY motif, implicated in constitutive activity of adrenoceptors when mutated, was also present in each model [57].

5.2. Docking results

The absence of a PI feature in the α_{1b} pharmacophore is a very interesting result, as it appears from our preliminary docking studies that the positively charged nitrogen is not as important for binding to the α_{1b} pocket as may have been expected. The archetypal α_1 -AR antagonist prazosin (32) was docked into optimised homology models of each of the three α_1 -AR subtypes. When prazosin was docked into an optimised α_{1a} homology model, the best docking energy was -12.5 . Prazosin did not exhibit the PI nitrogen–aspartate interaction expected of a ligand in complex with an adrenoceptor. This is,

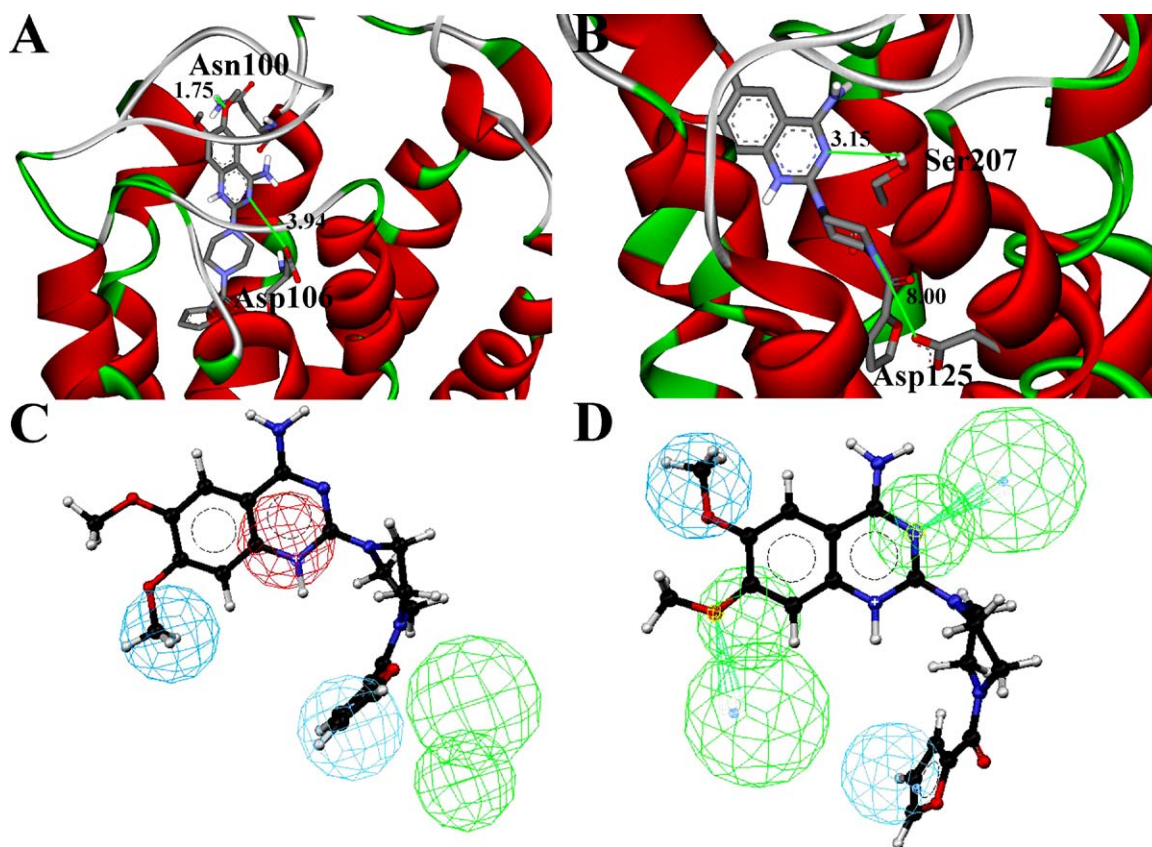


Fig. 4. (A) Prazosin docked into α_{1a} -AR. The shortest distance between Asp106 carbonyl O and any N of prazosin is 3.94 Å. (B) Prazosin docked into α_{1b} -AR. The shortest distance between Asp125 carbonyl O and any N of prazosin is 8.00 Å. (C) The α_{1a} pharmacophore mapped onto prazosin. The HBA feature does not map to any part of the structure. (D) The α_{1b} pharmacophore mapped onto prazosin. All four features map to the structure. Coloured spheres are the same as in Fig. 2.

however, in agreement with the finding that only class I antagonists map the PI feature in the α_{1a} pharmacophore. The shortest distance between the carbonyl oxygens of Asp106 and the closest nitrogen of prazosin was 3.94 Å (Fig. 4A). The lowest energy cluster of docking results for prazosin in α_{1b} consisted of 20 members and was at $E_{\text{dock}} - 11.8$. This cluster was found to bind in the region of conserved serine residues and did not exhibit an interaction between a PI nitrogen and the universally conserved aspartate. The shortest distance between the carbonyl oxygens of Asp125 and the closest nitrogen of prazosin was 8.00 Å (Fig. 4B). When docked into the α_{1d} homology model, prazosin was never found within the binding pocket, instead it was found at various places outside the helical bundle.

The α_{1d} -selective antagonist **66** was also docked into the three α_1 -AR models to explore the size difference question. When docked in α_{1a} , **66** did exhibit a charge-reinforced interaction between the PI nitrogen and carbonyl oxygen of Asp106 with N → O distance of 2.85 Å and N–H...O angle of 118.8°. The lowest energy cluster consisted of seven members at $E_{\text{dock}} - 14$. When docked in α_{1b} , no interaction between the PI nitrogen and Asp125 could be observed in any of the orientations and the antagonist again interacted with the region of the serine residues. The lowest energy cluster at $E_{\text{dock}} - 13.2$ consisted of 22 members. Similarly to prazosin docking in the α_{1d} model, **66** was never found to dock within the helical bundle.

These were intriguing results as they appear to agree with the average molecular weights of the training sets. Visual inspection of the optimised homology models indicates that this size difference between binding pockets is indeed present. We measured the distance between C $_{\alpha}$ of the universally conserved Asp residue and one of the conserved serines thought to be essential for binding of ligands. Surprisingly, this distance was essentially identical between the three models: α_{1a} , 12.65 Å; α_{1b} , 12.87 Å; α_{1d} , 12.88 Å. However, the α_{1d} pocket appears much more crowded than the other two pockets, due to the orientation of large, hydrophobic residues, while the α_{1a} pocket appears the least crowded of the three.

6. Conclusions

The α_{1a} pharmacophore consists of four features, HBA, Hal, Har, PI and is representative of antagonists with at least 100-fold selectivity over the α_{1b} receptor and 40-fold selectivity over α_{1d} . The training set for this pharmacophore included the two classes of antagonists as described by Klabunde and Evers, as well as structurally different compounds, which fitted into neither classification. The resultant pharmacophore was, however, weighted towards the class I antagonists, as they show higher selectivity and affinity than other antagonists.

The α_{1b} pharmacophore was generated from antagonists showing selectivity over the other two subtypes, which were predominantly prazosin analogues. This pharmacophore did not include a PI feature, as may have been expected, but included 2× HBA, Har and Hal features. The failure of Catalyst to assign a PI feature to the α_{1b} pharmacophore was

corroborated by the docking studies, which showed that ligands failed to undergo the interaction with the charged aspartate residue in the receptor cavity.

A five-feature pharmacophore was generated from those α_{1d} antagonists, which were 100-fold selective over α_{1a} and 40-fold selective over α_{1b} receptors. The pharmacophore consisted of HBA, 2× Hal, Har and PI features. The training set was heavily populated with analogues of BMY-7378, as these compounds are the only antagonists available which exhibit the appropriate type of selectivity. Despite this limitation of the training set, the pharmacophore was able to accurately predict the affinities of structurally distinct antagonists within a test set.

Preliminary docking studies were conducted using the archetypal α_1 -AR antagonist prazosin and the α_{1d} -selective antagonist **66** in optimised homology models of the three α_1 -AR subtypes. We found that the interaction between the PI nitrogen of prazosin and the negatively charged Asp did not occur in any of the models, whereas the interaction was observed for **66** in α_{1a} -AR. Inspection of the binding pockets indicates that, in agreement with the sizes of the antagonists in the training sets, the α_{1d} pocket is the smallest, the α_{1a} -AR pocket is the largest and the α_{1b} -AR pocket lies in between. As expected, antagonists bind close to the conserved Asp in the α_{1a} -AR binding pocket. However, in the α_{1b} -AR binding pocket, binding of antagonists close to the conserved Asp appears to be unfavourable, forcing ligands towards the conserved serines on helix V.

References

- [1] B. Civantos Calzada, A.A. De Artinano, Alpha-adrenoceptor subtypes, *Pharmacol. Res.* 44 (3) (2001) 195–208.
- [2] T. Klabunde, G. Hessler, Drug design strategies for targeting G-protein-coupled receptors, *ChemBioChem* 375 (2002) 261–276.
- [3] D. Giardina, M. Crucianelli, R. Romanelli, A. Leonardi, E. Poggesi, C. Melchiorre, Synthesis and biological profile of the enantiomers of [4-(4-amino-6,7-dimethoxyquinazolin-2-yl)-*cis*-octahydroquinoxalin-1-yl]furan-2-ylmethanone (cyclazosin), a potent competitive α_{1B} -adrenoceptor antagonist, *J. Med. Chem.* 39 (23) (1996) 4602–4607.
- [4] J.B. Bremner, B. Coban, R. Griffith, Pharmacophore development for antagonists at α_1 adrenergic receptor subtypes, *J. Comput. Aided Mol. Des.* 10 (6) (1996) 545–547.
- [5] J.B. Bremner, B. Coban, R. Griffith, K.M. Groenewoud, B. Yates, Ligand design for α_1 -adrenoceptor subtype selective antagonists, *Bioorg. Med. Chem.* 8 (2000) 201–214.
- [6] R. Barbaro, L. Betti, M. Botta, F. Corelli, G. Giannaccini, L. Maccari, F. Manetti, G. Strappaghetti, S. Corsano, Synthesis, biological evaluation, and pharmacophore generation of new pyridazinone derivatives with affinity toward α_1 - and α_2 -adrenoceptors, *J. Med. Chem.* 44 (2001) 2118–2132.
- [7] H. Fang, J.-F. Lu, L. Xia, Constructing biophore of uroselective α_1 -adrenoceptor antagonist, *J. Chin. Pharm. Sci.* 12 (4) (2003) 188–191.
- [8] G. Romeo, L. Materia, F. Manetti, A. Cagnotto, T. Mennini, F. Nicoletti, M. Botta, F. Russo, K.P. Minneman, New pyrimido[5,4-*b*]indoles as ligands for α_1 -adrenoceptor subtypes, *J. Med. Chem.* 46 (2003) 2877–2894.
- [9] M.-Y. Li, K.-C. Tsai, L. Xia, Pharmacophore identification of α_{1a} -adrenoceptor antagonists, *Bioorg. Med. Chem. Lett.* 15 (2005) 657–664.
- [10] T. Klabunde, A. Evers, GPCR antitarget modeling: pharmacophore models for biogenic amine binding GPCRs to avoid GPCR-mediated side effects, *ChemBioChem* 6 (2005) 876–889.

- [11] D.S. Goodsell, A.J. Olson, Automated docking of substrates to proteins by simulated annealing, *Proteins: Str. Func. Genet.* 8 (1990) 195–202.
- [12] G.M. Morris, D.S. Goodsell, R. Huey, A.J. Olson, Distributed automated docking of flexible ligands to proteins: parallel applications of AutoDock 2.4, *J. Comput. Aided Mol. Des.* 10 (1996) 293–304.
- [13] G.M. Morris, D.S. Goodsell, R.S. Halliday, R. Huey, W.E. Hart, R.K. Belew, A.J. Olson, Automated docking using a Lamarckian genetic algorithm and an empirical binding free energy function, *J. Comput. Chem.* 19 (1998) 1639–1662.
- [14] T. Balle, J. Perregaard, M.T. Ramirez, A.K. Larsen, K.K. Soby, T. Liljefors, K. Andersen, Synthesis and structure-affinity relationship investigations of 5-heteroaryl-substituted analogues of the antipsychotic serindole. A new class of highly selective α_1 adrenoceptor antagonists, *J. Med. Chem.* 46 (2003) 265–283.
- [15] M. Eltze, R. Boer, M.C. Michel, P. Hein, R. Testa, W.-R. Ulrich, N. Kolassa, K.H. Sanders, In vitro and in vivo uroselectivity of B8805-033, an antagonist with high affinity at prostatic α_{1a} - vs α_{1b} - and α_{1d} -adrenoceptors, *N.-S. Arch. Pharmacol.* 363 (2001) 649–662.
- [16] A.P.D.W. Ford, T.J. Williams, D.R. Blue, D.E. Clarke, α_1 -Adrenoceptor classification: sharpening Occam's razor, *Trends Pharmacol. Sci.* 15 (6) (1994) 167–170.
- [17] D. Giardina, M. Crucianelli, C. Melchiorre, C. Taddei, R. Testa, Receptor binding profile of cyclazosin, a new α_{1b} -adrenoceptor antagonist, *Eur. J. Pharmacol.* 287 (1) (1995) 13–16.
- [18] D. Giardina, O. Polimanti, G. Sagratini, P. Angeli, U. Gulini, G. Marucci, C. Melchiorre, E. Poggesi, A. Leonardi, Searching for cyclazosin analogues as α_{1b} -adrenoceptor antagonists, *Il Farmaco* 58 (2003) 477–487.
- [19] B. Kenny, S. Ballard, J. Blagg, D. Fox, Pharmacological options in the treatment of benign prostatic hyperplasia, *J. Med. Chem.* 40 (9) (1997) 1293–1315.
- [20] H. Khatuya, R.H. Hutchings, G.-H. Kuo, V.L. Pulito, L.K. Jolliffe, X. Li, W.V. Murray, Arylpiperazine substituted heterocycles as selective α_{1a} adrenergic antagonists, *Bioorg. Med. Chem. Lett.* 12 (2002) 2443–2446.
- [21] H. Khatuya, V.L. Pulito, L.K. Jolliffe, X. Li, W.V. Murray, Novel thiophene derivatives for the treatment of benign prostatic hyperplasia, *Bioorg. Med. Chem. Lett.* 12 (2002) 2145–2148.
- [22] H.K. King, A.S. Goetz, S.D.C. Ward, D.L. Saussy Jr., *Soc. Neuro. Abs.* 20 (1994) 526.
- [23] M.J. Konkel, J.M. Wetzel, M. Cahir, D.A. Craid, T.A. Branchek, S.A. Noble, C. Gluchowski, Discovery of antagonists selective for the α_1 adrenoceptor, in: *Book of Abstracts*, 216th ACS National Meeting, MEDI-129, Boston, August 23–27, 1998.
- [24] G.-H. Kuo, C. Prouty, W.V. Murray, V. Pulito, L. Jolliffe, P. Cheung, S. Varga, M. Evangelisto, J. Wang, Design, synthesis, and structure-activity relationships of phthalimide-phenylpiperazines: a novel series of potent and selective α_{1a} -adrenergic receptor antagonists, *J. Med. Chem.* 43 (11) (2000) 2183–2195.
- [25] G.-H. Kuo, C. Prouty, W.V. Murray, V. Pulito, L. Jolliffe, P. Cheung, S. Varga, M. Evangelisto, C. Shaw, Design, synthesis and biological evaluation of pyridine-phenylpiperazines: a novel series of potent and selective α_{1a} -adrenergic receptor antagonist, *Bioorg. Med. Chem.* 8 (2000) 2263–2275.
- [26] A. Leonardi, D. Barlocco, F. Montesanto, G. Cignarella, G. Motta, R. Testa, E. Poggesi, M. Seeber, P.G. De Benedetti, F. Fanelli, Synthesis, screening, and molecular modeling of new potent and selective antagonists at the α_{1d} -adrenergic receptor, *J. Med. Chem.* 47 (2004) 1900–1918.
- [27] X. Li, W.V. Murray, L. Jolliffe, V. Pulito, Novel arylpiperazines as selective α_1 -adrenergic receptor antagonists, *Bioorg. Med. Chem. Lett.* 10 (2000) 1093–1096.
- [28] X. Li, K.A. McCoy, W.V. Murray, L. Jolliffe, V. Pulito, Novel heterocycles as selective α_1 -adrenergic receptor antagonists, *Bioorg. Med. Chem. Lett.* 10 (2000) 2375–2377.
- [29] M.A. Patane, A.L. Scott, T.P. Broten, R.S.L. Chang, R.W. Ransom, J. DiSalvo, C. Forray, M.G. Bock, 4-Amino-2-[4-[1]-(benzyloxycarbonyl)-2(S)-[(1,1-dimethylethyl)amido]carbonyl]-piperazinyl]-6,7-dimethoxyquinazoline (L-765,314): a potent and selective α_{1b} -adrenergic receptor antagonist, *J. Med. Chem.* 41 (8) (1998) 1205–1208.
- [30] D.W. Phife, R.A. Ramos, M. Feng, I. King, S.P. Gunasekera, A. Wright, M. Patel, J.A. Pachter, S.J. Coval, Marine sponge bis(indole) alkaloids that displace ligand binding to α_1 -adrenergic receptors, *Bioorg. Med. Chem. Lett.* 6 (17) (1996) 2103–2106.
- [31] M. Rosini, A. Antonello, A. Cavalli, M.L. Bolognesi, A. Minarini, G. Marucci, E. Poggesi, A. Leonardi, C. Melchiorre, Prazosin-related compounds. Effect of transforming the piperazinylquinazoline moiety into an aminomethyltetrahydroacridine system on the affinity for α_1 -adrenoceptors, *J. Med. Chem.* 46 (2003) 4895–4903.
- [32] R. Testa, L. Guarneri, P. Angelico, E. Poggesi, C. Taddei, G. Sironi, D. Colombo, A.C. Sulpizio, D.P. Naselsky, J.P. Hieble, A. Leonardi, Pharmacological characterization of the uroselective α_1 -antagonist Rec 15/2739 (SB 216469): role of the α_1 -adrenoceptor in tissue selectivity, part II., *J. Pharmacol. Exp. Ther.* 281 (3) (1997) 1284–1293.
- [33] Catalyst 4.9 User Guide and On-line Help, Accelrys Inc., San Diego, CA, USA, 2003.
- [34] A. Smellie, S.L. Teig, P. Towbin, Poling: promoting conformational variation, *J. Comp. Chem.* 16 (1995) 171–187.
- [35] A. Smellie, S.D. Kahn, S.L. Teig, Analysis of conformational coverage 1. Validation and estimation of coverage, *J. Chem. Inf. Comp. Sci.* 35 (1995) 285–294.
- [36] A. Smellie, S.D. Kahn, S.L. Teig, Analysis of conformational coverage 2. Applications of conformational models, *J. Chem. Inf. Comp. Sci.* 35 (1995) 295–304.
- [37] M. Cocchi, M.C. Menziani, F. Fanelli, P.G. De Benedetti, Theoretical quantitative structure-activity relationship analysis of congeneric and non-congeneric α_1 -adrenoceptor antagonists: a chemometric study, *J. Mol. Struct. (Theochem)* 331 (1–2) (1995) 79–93.
- [38] P.G. De Benedetti, M. Cocchi, M.C. Menziani, F. Fanelli, Theoretical quantitative size and shape activity and selectivity analyses of 5-HT_{1A} serotonin and α_1 -adrenergic receptor ligands, *J. Mol. Struct. (Theochem)* 305 (1994) 101–110.
- [39] P. Venturelli, M.C. Menziani, M. Cocchi, F. Fanelli, P.G. De Benedetti, Molecular modelling and quantitative structure-activity relationship analysis using theoretical descriptors of 1,4-benzodioxan (WB-4101) related compounds α_1 -adrenergic antagonists, *J. Mol. Struct. (Theochem)* 276 (1992) 327–340.
- [40] M. Peitsch, Protein modeling by E-mail, *Biotechnology* 13 (1995) 658–660.
- [41] M. Peitsch, ProMod and Swiss-Model: internet-based tools for automated comparative protein modelling, *Biochem. Soc. Trans.* 24 (1996) 274–279.
- [42] N. Geux, M. Peitsch, SWISS-MODEL and the Swiss-PdbViewer: an environment for comparative protein modelling, *Electrophoresis* 18 (1997) 2714–2723.
- [43] L. Oliveira, T. Hulsen, D. Lutje Hulsik, A.C.M. Paiva, G. Vriend, Heavier-than-air flying machines are impossible, *FEBS Lett.* 564 (3) (2004) 269–273.
- [44] H. Li, J. Sutter, R. Hoffmann, HypoGen: an automated system for generating 3D predictive pharmacophore models, in: O. Guner (Ed.), *Pharmacophore Perception, Development, and Use in Drug Design*, International University Line, La Jolla, CA, USA, 2000, pp. 171–187.
- [45] J. Sutter, O. Guner, R. Hoffmann, H. Li, M. Waldman, Effect of variable weights and tolerances on predictive model generation, in: O. Guner (Ed.), *Pharmacophore Perception, Development, and Use in Drug Design*, International University Line, La Jolla, CA, USA, 2000, pp. 501–511.
- [46] P.G. De Benedetti, M.C. Menziani, G. Rastelli, M. Cocchi, Molecular orbital study of the nitrogen basicity of prazosin analogues in relation to their α_1 -adrenoceptor binding affinity, *J. Mol. Struct. (Theochem)* 233 (1991) 343–351.
- [47] C. Bolchi, P. Catalano, L. Fumagalli, M. Gobbi, M. Pallavicini, A. Pedreti, L. Villa, G. Vistoli, E. Valoti, Structure-affinity studies for a novel series of homochiral naphtho and tetrahydronaphtho analogues of α_1 antagonist WB-4101, *Bioorg. Med. Chem.* 12 (2004) 4937–4951.
- [48] Y. Madrero, M. Elorriaga, S. Martinez, M.A. Noguera, B.K. Cassels, P. D'Ocon, D.M. Ivorra, A possible structural determinant of selectivity of boldine and derivatives for the α_{1A} -adrenoceptor subtype, *Br. J. Pharmacol.* 119 (8) (1996) 1563–1568.

- [49] C. Melchiorre, P. Angeli, M.L. Bolognesi, A. Chiarini, D. Giardina, U. Gulini, A. Leonardi, G. Marucci, A. Minarini, M. Pigni, α_1 -Adrenoceptor antagonists bearing a quinazoline or a benzodioxane moiety, *Pharm. Acta Helv.* 74 (2–3) (2000) 181–190.
- [50] M.D. Meyer, R.J. Altenbach, H. Bai, F.Z. Basha, W.A. Carroll, J.F. Kerwin Jr., S.A. Lebold, E. Lee, J.K. Pratt, K.B. Sippy, K. Tjetje, M.D. Wendt, M.E. Brune, S.A. Buckner, A.A. Hancock, I. Drizin, Structure-activity studies for a novel series of bicyclic substituted hexahydrobenz[e]isoindole α_{1a} -adrenoceptor antagonists as potential agents for the symptomatic treatment of benign prostatic hyperplasia, *J. Med. Chem.* 44 (2001) 1971–1985.
- [51] V.L. Pulito, X. Li, S.S. Varga, L.S. Mulcahy, K.S. Clark, S.A. Halbert, A.B. Reitz, W.V. Murray, L.K. Jolliffe, An investigation of the uroselective properties of four novel α_{1a} -adrenergic receptor subtype-selective antagonists, *J. Pharmacol. Exp. Ther.* 294 (1) (2000) 224–229.
- [52] W. Quaglia, M. Pigni, A. Piergentili, M. Giannella, F. Gentili, G. Marucci, A. Carrieri, A. Carotti, E. Poggesi, A. Leonardi, C. Melchiorre, Structure-activity relationships in 1,4-benzodioxan-related compounds. 7. Selectivity of 4-phenylchroman analogues for α_1 -adrenoreceptor subtypes, *J. Med. Chem.* 45 (8) (2002) 1633–1643.
- [53] W.A. Carroll, K.B. Sippy, T.A. Esbenshade, S.A. Buckner, A.A. Hancock, M.D. Meyer, Two novel and potent 3-[(*o*-methoxyphenyl)piperazinylethyl]-5-phenylthieno[2,3-*d*]pyrimidine-2,4-diones selective for the α_{1d} receptor, *Bioorg. Med. Chem. Lett.* 11 (2001) 1119–1121.
- [54] P.G. De Benedetti, F. Fanelli, M.C. Menziani, M. Cocchi, R. Testa, A. Leonardi, α_1 -adrenoceptor subtype selectivity: molecular modelling and theoretical quantitative structure-affinity relationships, *Bioorg. Med. Chem.* 5 (5) (1997) 809–816.
- [55] F.N. Ko, J.H. Guh, S.M. Yu, Y.S. Hou, Y.C. Wu, C.M. Teng, (–)-Discretamine, a selective α_1D -adrenoceptor antagonist, isolated from *Fissistigma glaucescens*, *Br. J. Pharmacol.* 112 (4) (1994) 1174–1180.
- [56] R.A. Laskowski, M.A. MacArthur, D.S. Moss, J.M. Thornton, PROCHECK: a program to check the stereochemical quality of protein structures, *J. Appl. Crystallogr.* 26 (1993) 283–291.
- [57] P.J. Greasley, F. Fanelli, O. Rossier, L. Abuin, S. Cotecchia, Mutagenesis and modelling of the α_{1B} -adrenergic receptor highlight the role of the helix 3/helix 6 interface in receptor activation, *Mol. Pharmacol.* 61 (5) (2002) 1025–1032.